




Multimodal vibration suppression of nonlinear Euler–Bernoulli beam by multiple time-delayed vibration absorbers

Hao Meng · Xiuting Sun · Jian Xu  · Feng Wang

Received: 17 February 2021 / Accepted: 3 June 2021 / Published online: 1 July 2021
© Springer Nature B.V. 2021

Abstract For a nonlinear beam under broadband excitations, the multimodal nonlinear resonance phenomena will be induced. To suppress the multimodal nonlinear resonances, the multiple time-delayed vibration absorbers (TDVAs) are introduced. The optimal time-delayed parameters of the TDVAs are determined by the proposed multimodal equal-peak principle consisting of three design criteria. In the proposed three criteria, the stability criterion ensures the stability of the equilibrium state for the system; the extremes equal criterion figures out the time-delayed parameters to realize the equal resonance peaks around each concerned mode; the minimum peak criterion can obtain the optimal time-delayed parameters for the minimum resonance peaks. The results show that the TDVAs designed by the proposed multimodal equal-peak principle consisting of three criteria could simultaneously suppress the resonance peaks of the beam around multiple modes to the equal and minimum values. Besides, the equal resonance peaks are much lower than the absorbers without time-delayed feedback under the same mass constraint. The proposed TDVAs and the multimodal equal-peak

principle have wide application prospects in suppressing the multimodal vibrations for nonlinear continuous systems with broad frequency band and large amplitudes excitation in the fields of civil engineering and aerospace.

Keywords Nonlinear beam · Multimodal vibration suppression · Multimodal equal-peak principle · Multiple time-delayed vibration absorbers

1 Introduction

As a basic and efficient loading-bearing component, the elastic beam is widely used in many engineering applications, such as bridges and robotic arms [1, 2], etc. For elastic beams with light-damping property, multimodal resonances will be induced under broadband excitations [3, 4]. The wind tunnel tests and recorded field data for some long-span bridges around the world showed that the vortex vibration of bridges may occur in multiple modes [5–9]. Besides, some nonlinear phenomena induced by large-amplitude excitations, such as multiple steady-state, bifurcation and chaos, would reduce the service life and even lead to the failure for structures in engineering. Thus, an effective vibration suppression principle to suppress the multimodal resonances for nonlinear beams is worth investigating.

H. Meng · X. Sun · J. Xu (✉) · F. Wang
School of Aerospace Engineering and Applied Mechanics,
Tongji University, Shanghai 200092, China
e-mail: xujian@tongji.edu.cn

J. Xu
Shanghai Institute of Intelligent Science and Technology,
Tongji University, Shanghai 200092, China

In vibration suppression field, the dynamic vibration absorbers were applied to suppress the vibration of the primary system. The first linear undamped absorber was invented to suppress the resonance of a ship in 1909 [10]. It discovered that when the natural frequencies of the primary system and undamped absorber were equal, the resonance of the primary system could be suppressed to zero. However, two new resonance peaks with high values, which were close to the anti-resonance response, were introduced in the coupled system. Thus, the vibration suppression effect of linear undamped absorbers deteriorated rapidly for external excitations with frequency disturbance. To achieve broadband vibration suppression effects, Ormondroyd and Den Hartog introduced the damper in the linear tuned vibration absorber (LTVA) and proposed the “fixed-points theory” for its parameter optimization [11, 12]. The results showed that frequency response curves (FRCs) of the primary system passed through two fixed points for various damping coefficients of the LTVA. This characteristic could be applied to simplify the H_∞ optimization of the stiffness and damping coefficients for LTVA. Then many researchers were devoted to extend the fixed-points theory to different configurations or working conditions [13–17]. By attaching a LTVA designed by the fixed-points theory, the maximum response of the FRC for a single DOF linear primary system was minimized. In conclusion, the fixed-points theory was applied to suppress the single modal vibration of linear systems.

For nonlinear primary systems attached by a LTVA designed by the fixed-points theory, the two resonance peaks of the primary system were no longer minimum and would diverge from each other with increasing excitation amplitudes [18]. To tackle this challenge, Kerschen and his co-workers proposed the so-called equal-peak principle for the nonlinear tuned vibration absorber (NLTVA) [18–20]. Based on the proposed equal-peak principle, the restoring force function of the NLTVA should possess the same nonlinear forms and orders as the primary system. Sun et al. [21] revised the nonlinear stiffness coefficients of the NLTVA based on the equal-peak principle and explored its advantage in eliminating undesirable nonlinear phenomena. For nonlinear primary system with the NLTVA designed by the equal-peak principle, two resonance peaks of the primary system were approximately suppressed to the equal and

minimum value. In summary, LTVA and NLTVA could be applied to suppress the linear and nonlinear vibrations for the single modal vibration suppression problems.

For suppressing the multimodal vibrations of multiple DOF (MDOF) primary system, multiple absorbers could be applied by tuning each absorber per mode to be controlled [22–25]. Zhu et al. [22] studied the optimization problems of the multiple linear tuned vibration absorbers (LTVAs) for suppressing the multimodal vibrations of the linear plates. The results showed the multimodal vibration can be suppressed by using the optimized LTVAs. Raze and Kerschen [23] obtained the optimal structural parameters of the LTVAs by adopting the norm-homotopy optimization algorithm. It discovered that the multiple linear resonances were suppressed to the equal and minimum values in a broad frequency band that contained multiple modes. For suppressing the multiple nonlinear resonances of MDOF nonlinear primary systems, the multiple nonlinear tuned vibration absorbers (NLTVAs) were applied and the semi-analytical formula of structural parameters for NLTVAs was obtained by the equal-peak principle [24]. The numerical results indicated that multiple nonlinear resonance peaks of the primary system could be suppressed to approximately equal values. However, with the increase of force amplitude, a detached resonance curve (DRC) appeared and then merged with the main resonance curve (MRC). The merging phenomena would lead to the failure of the equal-peak property. In conclusion, most researchers studied the realization of the equal-peak principle with passive absorbers, but the limitations of passive absorbers on realizing the equal-peak principle were mainly in the following aspects. (i) The first is the contradiction between the vibration suppression performance (resonance peak values of the primary system) and the mass ratio of the absorber. The results of the equal-peak principle [15] showed that the resonance peak of the primary system is the monotonically decreasing function of the mass ratio of the absorber, which indicated that the heavier absorber should be installed to suppress the resonance peaks to lower values. However, the absorber’s mass ratio cannot be too heavy due to some constraints in practical engineering fields. (ii) The second is the contradiction between the designable requirements of absorber stiffness and the reality that the optimal

stiffness of the absorber is fixed [18, 26]. For example, a larger stiffness value than the optimal value designed by the equal-peak principle can improve the loading capacity of the absorber, but it will reduce the vibration suppression performance. (iii) The third is the contradiction between non-adjustable property for passive absorbers and variable external excitations. For a nonlinear primary system, the resonance frequency varied with the variation of excitation amplitudes. However, the structural parameters of passive absorbers are fixed and their vibration characteristics cannot be tuned according to the variation of external excitations. Thus, passive absorbers were not applicable for some nonlinear primary systems under variable frequency or amplitude excitations.

To tackle the aforementioned limitations of passive absorbers, active absorbers were adopted. Among various active absorbers, the time-delayed vibration absorber (TDVA) has received extensive attentions [27–37]. Compared with the traditional active absorbers, the TDVA has the following characteristics. (i) Time delay is inevitable in active control loops. It mainly comes from the process of limited transmission speed, filtering, on-line calculation and applying active force. Therefore, the mechanical model of the active control system with time delay is more accurate than that without time delay. (ii) The vibration control effect of the passive absorber is mainly realized by tuning the stiffness and damping properties. The previous studies of TDVA [30, 31, 35, 37] showed that time-delayed feedback can tune the equivalent stiffness and damping properties of the absorber. Thus, the physical meaning of TDVA is clear, the mechanical mechanism is intuitive and interpretable. (iii) In the time-delayed control loop, only part of the state variable feedback signal is needed. Since no additional state variable feedback signal is required, the noise amplification due to the derivative and the numerical error due to the integration can be avoided. (iv) The choice of the feedback control signal is flexible. The signal can be either displacement [35], velocity [38], or acceleration [30], which depends on the type of sensor, the convenience of signal measurement and the specific configuration of vibration absorbers. Therefore, TDVA has been widely applied in vibration suppression fields.

Most previous researches of TDVA focused on the frequency modulation mechanism for either linear [30, 31, 35] or nonlinear primary systems [37]. With

proper time-delayed parameters determined by the frequency modulation mechanism, the anti-frequency of the time-delayed system can be tuned equally with the excitation frequency and the response of the primary system can be suppressed to zero. Since the anti-frequency point was tunable with time-delayed feedback, TDVA can realize the broad frequency band vibration suppression effects. However, the suppressing of resonance responses was not considered for the frequency modulation mechanism. For the primary system with the TDVA designed by the frequency modulation mechanism, a small drift of excitation frequency will lead to a rapid increase of response magnitude. To handle this challenge, the TDVA is explored to generalize the equal-peak principle to single DOF nonlinear systems in our previous work [39]. In the generalization process, a new vibration suppression mechanism of TDVA is discovered, called amplitude modulation mechanism. The results showed that for nonlinear primary systems attached with TDVA designed by the equal-peak principle, the resonance peaks can be suppressed lower and the effective force amplitude range is extended larger than the passive LTVA and NLTVA. To sum up, with the proposed equal-peak principle, TDVA could be applied to suppress the single modal resonance response [39] and it is desirable to study the generalization of the proposed principle to suppress the multimodal nonlinear resonances of nonlinear beams.

For nonlinear beams under broadband excitations, nonlinear resonance phenomena will be induced around multiple modes, so the multiple resonances need to be simultaneously suppressed. Our previous work [39] showed that single resonance of the primary system was suppressed to two equal resonance peaks with much lower values by a single TDVA based on the equal-peak principle. Thus, multiple TDVAs are applied and the equal-peak principle is extended to suppress the multiple resonances for a nonlinear beam, called multimodal equal-peak principle in this study. The layout of this paper is arranged as follows. In Sect. 2, the mechanical model of a nonlinear beam attached by the TDVAs is given and the optimization objective of the multimodal equal-peak principle is formulated. The optimization procedure of the multimodal equal-peak principle is illustrated in Sect. 3 and two case studies are given to verify the vibration suppression performance for TDVAs. The conclusions of the present study are summarized in Sect. 4.

2 Mechanical model and optimization objective

2.1 Mechanical model

The primary system is a Euler–Bernoulli beam with geometrical nonlinearity as Fig. 1a. The geometrical nonlinearity follows the assumption of von Kármán type strain–displacement relation [3]. For the light-damped nonlinear beam subjected to excitations with broad frequency band and large amplitude, nonlinear resonances are easily induced around multiple modes. To suppress the multimodal nonlinear resonances of the beam to the minimum values, N absorbers are attached as Fig. 1b. The mechanical model is shown in Fig. 1.

As shown in Fig. 1a, the symbols E, I, ρ, A, c and l are the Young’s modulus, area moment of inertia, density, cross-sectional area, damping coefficients and length of the beam, respectively. $F_e = f \cos(\Omega t)$ is the external excitation applied on the beam at the location point s_f , with excitation amplitude f and frequency Ω . In Fig. 1b, the symbols m_i, k_i, c_i and s_i denote the mass, linear stiffness, damping coefficients and location point of i th TDVA, which is attached to suppress the resonance response around i th mode for the beam. The feedback signal of i th TDVA is adopted as the same form $g_i v_i(t - \tau_i)$, where g_i and τ_i are the control gain and time delay for the i th absorber, respectively. According to the theory of nonlinear Euler–Bernoulli beam [3], the equations governing the transverse displacements of the beam $w(s, t)$ and the absorbers $v_i(t)$ are written as

$$\begin{aligned} & \rho A \ddot{w}(s, t) + c \dot{w}(s, t) + EI w''''(s, t) \\ & - \frac{EA}{2I} w''(s, t) \int_0^l (w'(s, t))^2 ds \\ & + \sum_{i=1}^N m_i \ddot{v}_i(t) \delta(s - s_i) = F_e \delta(s - s_f), \\ & m_i \ddot{v}_i(t) + k_i [v_i(t) - w(s_i, t)] + c_i [\dot{v}_i(t) - \dot{w}(s_i, t)] \\ & - g_i v_i(t - \tau_i) = 0, \end{aligned} \tag{1}$$

where the nonlinear term $-\frac{EA}{2I} w'' \int_0^l (w')^2 ds$ is induced by the von Kármán type nonlinear strain–displacement relation assumption, $\delta(s - s_i)$ and $\delta(s - s_f)$ are the Dirac delta functions representing the concentrated force of the i th TDVA and the external excitation applied on the beam. The over dot and the prime denote the derivative with respect to time t and the spatial coordinate s , respectively.

The dimensionless truncation equations are derived by applying the Galerkin truncation and the dimensionless process (See Appendix A for details)

$$\begin{aligned} & \ddot{x}_p + 2\zeta_p \dot{x}_p + \lambda_p^2 x_p + f_{nl,p} + \sum_{i=1}^N \mu_i \ddot{y}_i(t) \phi_p(s_i) \\ & = f_p, p = 1, 2, \dots, P, \\ & \ddot{y}_i + \beta_i^2 \left[y_i - \sum_{p=1}^P \phi_p(s_i) x_p \right] + 2\gamma_i \beta_i \left[\dot{y}_i - \sum_{p=1}^P \phi_p(s_i) \dot{x}_p \right] \\ & - \lambda_i^2 g_i v_i(t - \tau_i) = 0, i = 1, 2, \dots, N, \end{aligned} \tag{2}$$

where $x_p, \phi_p(s)$ are the p th dimensionless generalized coordinate and linear mode shape of the beam, y_i and μ_i are the dimensionless displacement and mass ratio of i th TDVA, λ_p and ζ_p are the p th modal dimensionless frequency and damping ratio of the beam, β_i and γ_i

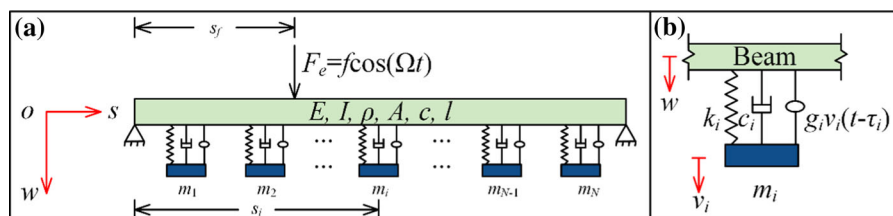


Fig. 1 The schematic of **a** the Euler–Bernoulli beam with geometrical nonlinearity attached by TDVAs, **b** the i th TDVA

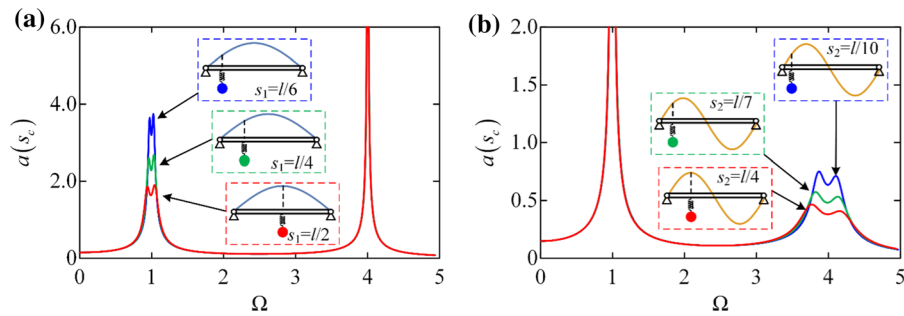


Fig. 2 FRCs of the linear beam with a single LTVA at different locations designed by the fixed-points theory targeted for the **a** first mode, **b** second mode as $P = 2$

are the dimensionless frequencies and damping ratio of i th absorber. $f_{nl,p}$ and f_p are the p th nonlinear restoring force and the modal force of the beam, which are written as

$$f_{nl,p} = -\frac{f^2 EA}{2lK_1^3} \sum_{p_1=1}^P \sum_{p_2=1}^P \sum_{p_3=1}^P x_{p_1} x_{p_2} x_{p_3} \int_0^l \phi_{p_3}''(s) \phi_p(s) \left(\int_0^l \phi_{p_1}'(s) \phi_{p_2}'(s) ds \right) ds, f_p = \phi_p(s_f) \cos(\Omega t). \tag{3}$$

Equation (2) can be rewritten in a compact form

$$\mathbf{M}\ddot{\mathbf{X}} + \mathbf{C}\dot{\mathbf{X}} + \mathbf{K}\mathbf{X} + \mathbf{F}_n + \mathbf{G}_\tau = \mathbf{F}, \tag{4}$$

where $\mathbf{X} = [x_1, \dots, x_p, y_1, \dots, y_N]^T$ is the displacement vector; \mathbf{M} , \mathbf{C} and \mathbf{K} are the coefficient matrices of the mass, damping and stiffness, respectively; \mathbf{F}_n is the vector of the nonlinear restoring forces generated by the nonlinear term of the beam. \mathbf{G}_τ is the vector of the time-delayed feedback force. \mathbf{F} is the external force vector applied on the beam.

The objective of the multimodal equal-peak principle in this study is to simultaneously suppress the multiple resonance peaks of the frequency response curve (FRC) for the nonlinear beam to equal and minimum values. The resonance peaks are local maximum points of FRC, thus the FRC should be derived firstly. By applying the Averaging Method, the FRC of the beam at the location s_c is obtained as (See [Appendix B](#) for details)

$$a(s_c) = \sqrt{\left(\sum_{p=1}^P A_{p,1} \phi_p(s_c) \right)^2 + \left(\sum_{p=1}^P A_{p,2} \phi_p(s_c) \right)^2}, \tag{5}$$

where $A_{p,1}, A_{p,2}, p = 1, 2, \dots, P, i = 1, 2, \dots, N$ are the fundamental harmonic coefficients of the nonlinear beam.

2.2 Optimization objective

In the subsequent analysis, the beam is assumed as homogenous elastic with the mass density $\rho = 7860 \text{ kg/m}^3$, Young’s modulus $E = 210 \text{ GPa}$, length $l = 1 \text{ m}$, cross-section area $A = 0.00103 \text{ m}^2$, the moment inertia $I = 1.71 \times 10^{-6} \text{ m}^4$ [40] and the damping ratio $\zeta_p = 0.1\%$. To have a common base for the comparison, the total mass of the absorbers is $\mu = 0.01$, the force excitation is applied at $s_f = 9l/10$ and the FRC is computed at the location point $s_c = l/10$.

2.2.1 LTVAs coupled to the linear beam

When subjected to small amplitude excitations, the nonlinear beam degenerates to a linear one since its nonlinearity is not activated. Besides, when the excitation frequency is near i th natural frequency of the beam, its vibration is dominated by the i th mode and the effect of other modes can be neglected. First, we apply a linear analysis to gain an insight into the single modal vibration suppression performance for the linear beam. The i th modal vibration of the linear beam can be suppressed by the i th LTVA without

time-delayed feedback. Thus, Eq. (2) degenerates to a two DOF system

$$\begin{aligned} \ddot{x}_i + 2\zeta_i \dot{x}_i + \lambda_i^2 x_i + \mu_i \ddot{y}_i(t) \phi_i(x_i) &= f_i, \\ \ddot{y}_i + \beta_i^2 [y_i - \phi_i(s_i) x_i] + 2\gamma_i \beta_i [\dot{y}_i - \phi_i(s_i) \dot{x}_i] &= 0. \end{aligned} \tag{6}$$

Equation (6) has the same form as the equations of motions for a single lumped mass primary system controlled by an absorber [26]. Based on the “fixed-points theory”, the equivalent mass ratio, stiffness and damping coefficients of i th LTVA are determined as

$$\begin{aligned} \hat{\mu}_i &= \mu_i \phi_i^2(s_i), \\ \beta_i &= \frac{2\lambda_i}{1 + \hat{\mu}_i} \sqrt{\frac{2(16 + 23\hat{\mu}_i + 9\hat{\mu}_i^2 + 2(2 + \hat{\mu}_i)\sqrt{4 + 3\hat{\mu}_i})}{3(64 + 80\hat{\mu}_i + 27\hat{\mu}_i^2)}}, \\ \gamma_i &= \frac{1}{4} \sqrt{\frac{8 + 9\hat{\mu}_i - 4\sqrt{4 + 3\hat{\mu}_i}}{1 + \hat{\mu}_i}}. \end{aligned} \tag{7}$$

By attaching a LTVA designed by Eq. (7), two resonance peaks around the i th mode for the linear beam are suppressed to the equal minimum value as

$$a_i(s_c) = \frac{|\phi_i(s_f) \phi_i(s_c)| K_1}{K_i} \sqrt{\frac{2 + \hat{\mu}_i}{\hat{\mu}_i}}, \tag{8}$$

where K_i is the i th modal stiffness of the linear beam, $a_i(s_c)$ is a monotonically decreasing function that depends on $\hat{\mu}_i$. It indicates that for a fixed mass ratio of the LTVA, to suppress the peak amplitude of the beam around i th mode to its minimum value, the i th LTVA should be assembled at the maximum point of i th modal shape for the beam. Figure 2a, b show the FRCs of the linear beam with a single LTVA at different locations designed by Eq. (7) targeted for the first and second mode.

From Fig. 2, it can be seen that for the fixed mass ratio, the single LTVA located at the maximum of the i th linear mode shape could suppress the resonance peaks of the linear beam around i th mode to the equal and minimum values approximately. Besides, due to the damping and modal coupling effects of the beam, the two peaks either around the first and second modes are not strictly equal, but the vibration suppression performance of the LTVA is almost not affected.

To extend the fixed-points theory to the multimodal vibration suppression issue and suppress the peaks around multiple modes to the equal and minimum

values, multiple LTVAs should be assembled. The stiffness and damping coefficients of i th absorber, which targets for the i th mode of the beam, can be determined referring to Eq. (7) and their mass ratios are determined according to

$$\begin{aligned} a_i(s_c) &= a_{i+1}(s_c), i = 1, \dots, N - 1 \\ \sum_{i=1}^N \mu_i &= \mu, \end{aligned} \tag{9}$$

where the first equation is applied to ensure the multiple resonance peaks around each mode for the beam are equal and the second equation means the total mass ratio of the LTVAs is μ . Equations (7) and (9) form the generalized fixed-points theory of LTVAs for multimodal suppression problems. The FRCs of the linear beam with LTVAs designed by the generalized fixed-points theory for suppressing the resonances around two, three and four modes are shown in Fig. 3a, b and c, respectively.

Figure 3 illustrates the generalized fixed-points theory is applicable to suppress the multimodal vibration of the linear beam. By attaching LTVAs determined by Eqs. (7) and (9), the resonance peaks around multiple modes could be suppressed to equal and minimum values approximately. In the next section, the multimodal vibration suppression performance of LTVAs designed by the generalized fixed-points theory are explored for the nonlinear beam.

2.2.2 LTVAs coupled to the nonlinear beam

In this section, the nonlinearity of the beam is considered, the multimodal vibration suppression performance of the LTVAs for the nonlinear beam is investigated. Figure 4 shows the FRCs of the nonlinear beam around the first two modes attached by two LTVAs with increasing force amplitudes for $P = 2$.

In Fig. 4a for $f = 30$ kN, the nonlinearity of the beam is not apparent and its FRC is similar to the linear beam in Fig. 3a. Then, with the increase of force amplitude, the nonlinear phenomena of the beam become more and more apparent. In Fig. 4b for $f = 90$ kN, the two peaks around the first and second modes are slightly different. In Fig. 4c for $f = 100$ kN and Fig. 4d for $f = 150$ kN, the two peaks around the second and first modes are completely detuned and the multiple steady-state phenomena occur, respectively.

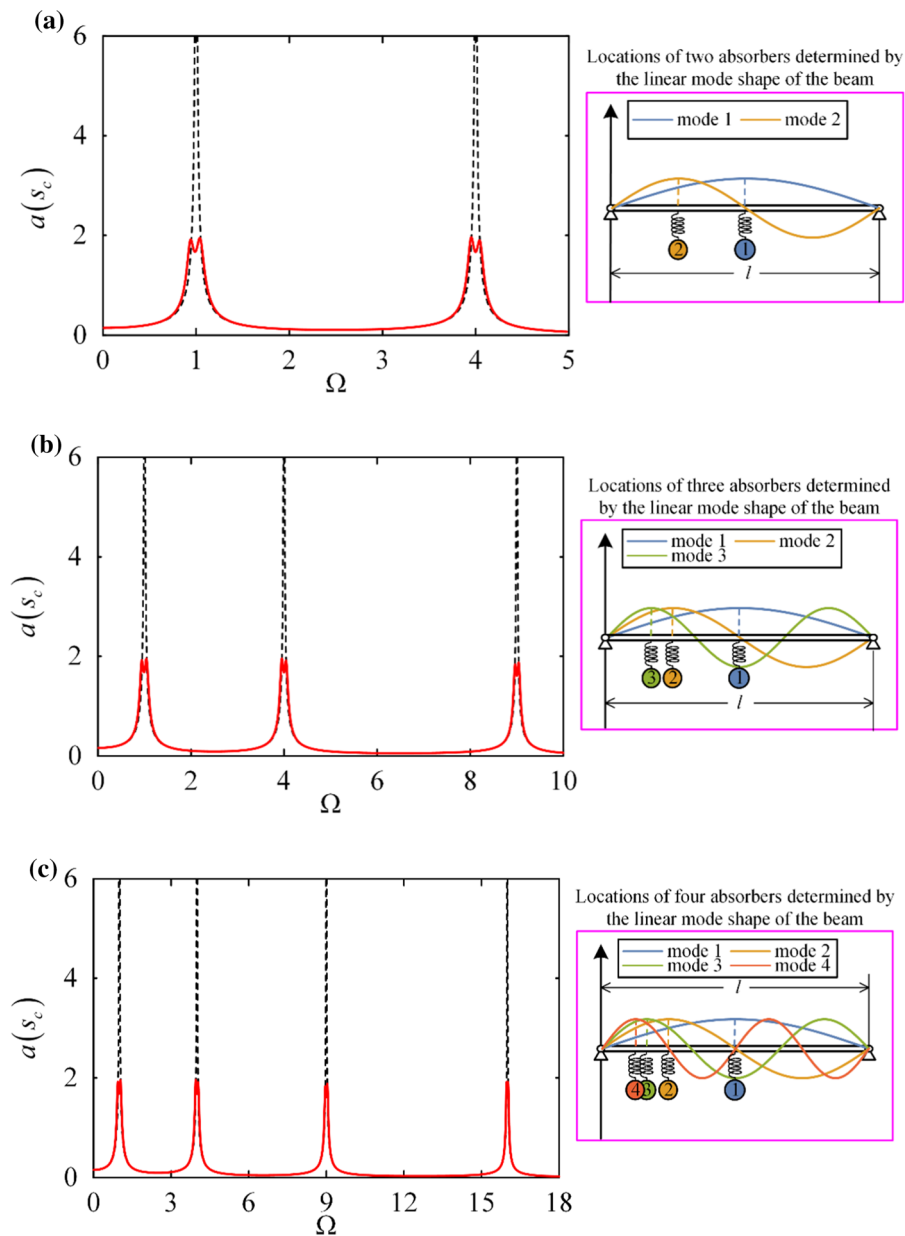


Fig. 3 FRCs of the linear beam with LTVAs designed by the generalized fixed-points theory targeted for the **a** first two modes as $P = 2$, **b** first three modes as $P = 3$, **c** first four modes as

$P = 4$. Red lines and black dashed lines are the FRCs with and without LTVAs. The locations of the four LTVAs are $s_1 = l/2$, $s_2 = l/4$, $s_3 = l/6$, $s_4 = l/8$, respectively

From the FRCs of the linear beam in Fig. 3 and the FRCs of the nonlinear beam with increasing excitation amplitudes in Fig. 4, the challenges of passive LTVAs designed by the fixed-points theory are revealed as follows. (i) As Eq. (8), the resonance peaks of the

linear beam depend on the mass ratio of the LTVAs and a larger mass ratio will lead to lower peaks. However, in practical engineering, the total absorbers' mass cannot be too heavy. (ii) As Eq. (7), the values of absorber's stiffness and damping coefficients are

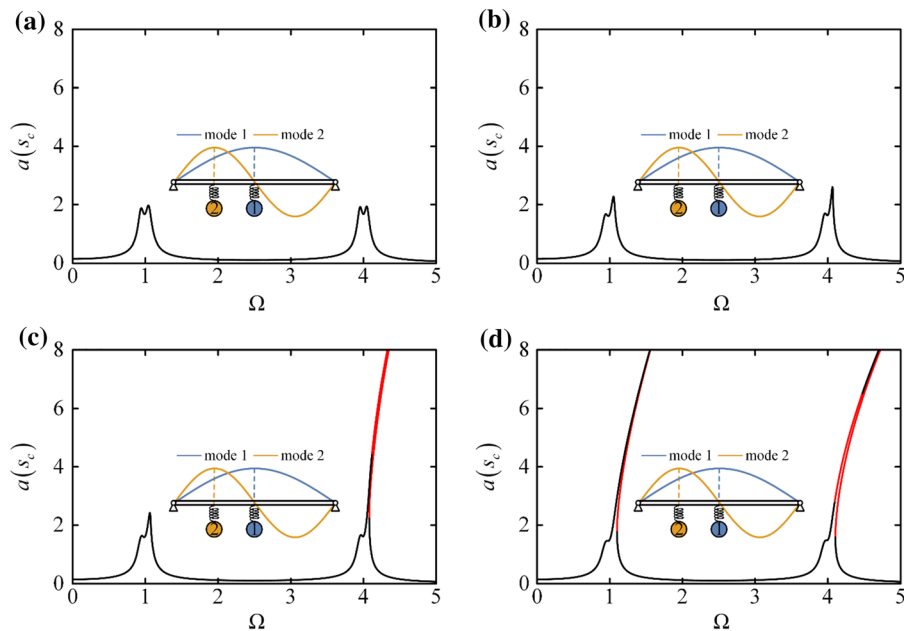


Fig. 4 FRCs of the nonlinear beam with LTVAs designed by the generalized fixed-points theory with Eq. (7) and (9) targeted for the first and second modes as $P = 2$, the black and red lines are the stable and unstable responses, respectively. **a** the two peaks are almost equal for the first and second modes at $f = 30$ kN; **b** the two peaks are slightly different for the first and second

modes at $f = 90$ kN; **c** the two peaks are completely detuned for the second mode at $f = 100$ kN; **d** the two peaks are completely detuned for the first and second modes at $f = 150$ kN. The locations of the two absorbers are $s_1 = l/2, s_2 = l/4$, respectively

single-valued functions of the absorber’s mass ratio. Thus, they are not designable for given mass ratios and assembly locations. For example, compared with the optimal stiffness of the LTVAs given in Eq. (7), a higher stiffness may reduce the vibration suppression performance and a lower stiffness may reduce the loading capacity. (iii) For nonlinear primary systems in this case, the resonance frequencies are dependent on the excitation amplitudes and the primary system presents a hardening behavior. However, Fig. 4 indicates that the vibration characteristics of passive LTVAs cannot be tuned with the variation of excitation amplitudes. Thus, passive LTVAs with the generalized fixed-points theory are not applicable to suppress the multimodal nonlinear vibrations for the nonlinear beam.

To handle the aforementioned limitations of the passive LTVAs and suppress the multimodal nonlinear resonances of the nonlinear beam, multiple time-delayed vibration absorbers (TDVAs) are adopted and the optimization objective of the multimodal equal-

peak principle is carried out. The objective is to suppress the resonance peaks around the concerned modes at the location s_c of a nonlinear beam to the equal and minimum values, which can be formulated as

$$\begin{aligned}
 &\text{Find } \mathbf{p}_\tau = \{g_i, \tau_i\} \text{ that satisfies} \\
 &\text{Min} \|a(s_c, \mathbf{p}, \mathbf{p}_\tau, \Omega)\|_\infty \\
 &\rightarrow \text{Min} \{ \text{Max} [a(s_c, \mathbf{p}, \mathbf{p}_\tau, \Omega_{2i-1}), a(s_c, \mathbf{p}, \mathbf{p}_\tau, \Omega_{2i})] \} \\
 &\rightarrow a(s_c, \mathbf{p}, \mathbf{p}_\tau, \Omega_{2i-1}) = a(s_c, \mathbf{p}, \mathbf{p}_\tau, \Omega_{2i}), i \in \Psi.
 \end{aligned}
 \tag{10}$$

In Eq. (10), $a(s_c, \mathbf{p}, \mathbf{p}_\tau, \Omega)$ is the FRC of the beam at the location s_c , $\mathbf{p} = \{\beta_i, \gamma_i, f\}$, $i \in \Psi$ is the vector that contains the structural parameters of the TDVAs and force amplitudes, $\mathbf{p}_\tau = \{g_i, \tau_i\}$, $i \in \Psi$ is the vector that contains control gains and time delays of the TDVAs, Ψ are the set of modes around which the resonance peaks are required to be suppressed, Ω_{2i-1} and Ω_{2i} are the resonance frequencies around the i th mode of the FRC. Due to the designable requirements

of the structural parameters of TDVAs, \mathbf{p} may be different from the optimal parameters of LTVAs designed by Eqs. (7 and 9), which is defined as $\mathbf{p}_0 = \{\beta_i^0, \gamma_i^0, f\}$, $i \in \Psi$.

3 Multimodal equal-peak principle with TDVAs for nonlinear beam

In this section, we carry out three criteria to realize the goal of multimodal equal-peak principle as Eq. (10) for the nonlinear beam, which simultaneously suppress the resonance peaks around multiple concerned modes Ψ to the equal and minimum values. First, the stability criterion restricts the time-delayed parameters \mathbf{p}_τ to the region in which the equilibrium state of the time-delayed system is stable. Then, the extremes equal criterion is carried out to figure out the time-delayed parameters \mathbf{p}_τ with which two resonance peaks around i th mode of the FRC are equal. Finally, considering that different time-delayed parameters \mathbf{p}_τ lead to peaks with different values, the minimum peak criterion is proposed to select the optimal \mathbf{p}_τ with the minimum resonance amplitudes.

The complete procedure, including the three criteria, is presented in Appendix C in detail. To illustrate the proposed procedure and the purpose of the three criteria, the resonances around the first and second modes are required to be suppressed in this section, thus the concerned modes are $\Psi = \{1, 2\}$. For simplicity, the first two modes of the beam are retained and two TDVAs are attached to minimize the resonances around the first two modes, thus $P = 2$ and $N = 2$. The matrix and vector of Eq. (4) for $P = 2$ and $N = 2$ are listed in Eqs. (26, 27, 28, 29, 30 and 31) in Appendix A. The total mass ratio of the TDVAs is $\mu = 0.01$, the same as the LTVAs in Sect. 2 to have a common base for the comparison. The optimal structural parameters of LTVAs determined by Eqs. (7 and 9) are $\mathbf{p}_0 = \{\beta_1^0, \beta_2^0, \gamma_1^0, \gamma_2^0, f\} = \{0.9813, 3.9962, 0.0838, 0.019, 0 \sim 10^5\}$. The structural parameters of TDVAs are adopted as $\mathbf{p} = \{\beta_1, \beta_2, \gamma_1, \gamma_2, f\} = \{1.5\beta_1^0, 1.5\beta_2^0, 0.3\gamma_1^0, 0.3\gamma_2^0, 0 \sim 10^5\}$.

3.1 Stability criterion

In the time-delayed loop, inappropriate time-delayed parameters destabilize the system and induce the

bifurcation, thus the stability criterion should be proposed to guarantee the stability of the equilibrium state. The stability of the equilibrium state can be determined by the sign of eigenvalues with the degenerated linear system. The characteristic equation of the linearized system of Eq. (4) is written as

$$\det[\mathbf{M}s^2 + \mathbf{C}s + \mathbf{K} + \mathbf{G}_\tau(\mathbf{p}_\tau)] = 0, \quad i \in \Psi, \quad (11)$$

where the expressions of the matrix are in Eqs. (26, 27, 28, 29, 30, 31 and 32) in Appendix A.

The eigenvalue of Eq. (11) has the form as $s = \alpha + i\omega_c$, where α and ω_c are the real and imaginary parts, respectively. The system is stable if all the eigenvalues have negative real parts. Therefore, time-delayed parameters $\mathbf{p}_\tau = \{g_i, \tau_i\}$, $i \in \Psi$ satisfy the following stability criterion

$$r_1 = \{\mathbf{p}_\tau | \text{Max}[\alpha(\mathbf{p}, \mathbf{p}_\tau)] < 0\}, \quad i \in \Psi. \quad (12)$$

Eq. (12) gives the first parameter design criterion for the multimodal equal-peak principle. Following Eq. (12), the system is stable with structural parameters \mathbf{p} and time-delayed parameters \mathbf{p}_τ , otherwise, the response of the system will diverge due to the existence of real part eigenvalues.

3.2 Extremes equal criterion

Inspired by the fact that in the linear case shown in Sect. 2.2.1, the two resonance peaks around i th mode of the linear beam are equal and minimum with the optimal LTVAs. Thus, the extremes equal criterion is proposed firstly to figure out the time-delayed parameters \mathbf{p}_τ that tune the two extreme points around i th mode equally. The resonances are extreme points of the FRC. According to the FRC of the beam $a(s_c)$ as Eq. (5) (see Appendix B for details), the frequencies of the extreme points around i th mode can be figured out with the first-order derivative of the FRC as

$$\begin{aligned} \frac{da(s_c)}{d\Omega} &= \frac{\left(\sum_{p=1}^P A_{p,1} \phi_p(s_c) \frac{dA_{p,1}}{d\Omega} + \sum_{p=1}^P A_{p,2} \phi_p(s_c) \frac{dA_{p,2}}{d\Omega} \right)}{\sqrt{\left(\sum_{p=1}^P A_{p,1} \phi_p(s_c) \right)^2 + \left(\sum_{p=1}^P A_{p,2} \phi_p(s_c) \right)^2}} \\ &= 0, \quad i \in \Psi, \end{aligned} \quad (13)$$

where $\frac{dA_{p,1}}{d\Omega}$ and $\frac{dA_{p,2}}{d\Omega}$ are computed by applying the

implicit differentiation to Eq. (35). The condition that the two extreme points around i th mode are equal can be formulated as

$$\begin{cases} \Gamma(\mathbf{v}_{2i-1}, \Omega_{2i-1}, \mathbf{p}, \mathbf{p}_\tau) = 0, & i \in \Psi, \\ \Gamma(\mathbf{v}_{2i}, \Omega_{2i}, \mathbf{p}, \mathbf{p}_\tau) = 0, & i \in \Psi, \\ \left. \frac{da(s_c, \mathbf{p}, \mathbf{p}_\tau, \Omega)}{d\Omega} \right|_{\Omega=\Omega_{2i-1}} = 0, \left. \frac{da(s_c, \mathbf{p}, \mathbf{p}_\tau, \Omega)}{d\Omega} \right|_{\Omega=\Omega_{2i}} = 0, & i \in \Psi, \\ a(s_c, \mathbf{p}, \mathbf{p}_\tau, \Omega_{2i-1}) = a(s_c, \mathbf{p}, \mathbf{p}_\tau, \Omega_{2i}). & i \in \Psi, \end{cases} \quad (14)$$

In Eq. (14), $\Gamma(\mathbf{v}, \Omega, \mathbf{p}, \mathbf{p}_\tau)$ is the amplitude modulation equation (see Appendix B in detail). The first and second equations obtain the harmonic response coefficients \mathbf{v}_{2i-1} and \mathbf{v}_{2i} at Ω_{2i-1} and Ω_{2i} , respectively. Combining the calculated \mathbf{v}_{2i-1} , \mathbf{v}_{2i} with Eq. (5), the response amplitudes at Ω_{2i-1} and Ω_{2i} are obtained as $a(s_c, \mathbf{p}, \mathbf{p}_\tau, \Omega_{2i-1})$ and $a(s_c, \mathbf{p}, \mathbf{p}_\tau, \Omega_{2i})$. The third and fourth equations ensure that $a(s_c, \mathbf{p}, \mathbf{p}_\tau, \Omega_{2i-1})$ and $a(s_c, \mathbf{p}, \mathbf{p}_\tau, \Omega_{2i})$ are two extreme points around i th mode. The fifth equation guarantees that the two extreme points have the same value. Eq. (14) can be rewritten as a concise form

$$r_{2,a} = \{\mathbf{p}_\tau | a(s_c, \mathbf{p}, \mathbf{p}_\tau, \Omega_{2i-1}) = a(s_c, \mathbf{p}, \mathbf{p}_\tau, \Omega_{2i})\} \cap r_1, i \in \Psi. \quad (15)$$

By applying Eq. (15) for i th mode, the obtained time-delayed parameters can tune the two extreme points equally around the i th mode. Figures 5 and 6 depict the time-delayed parameters obtained by Eq. (15) and corresponding FRCs for the first and second mode at $f = 200$ kN, respectively.

The time-delayed parameters in Fig. 5a are obtained by Eq. (15) for the first mode at $\tau_2 = 0.0079636$. With the time-delayed parameters shown in Fig. 5a, the 3D diagrams of FRCs are depicted in Fig. 5b. The 3D diagrams in Fig. 5b illustrate that in this case, the FRC consists of the main resonance curve (MRC, defines as the lower branch of FRC) and the detached resonance curves (DRCs, defines as the upper branches of FRCs) around the first and second modes. The DRCs are induced by the system nonlinearity under large amplitude excitation. From the 3D diagram of FRCs around the first mode shown in Fig. 5b, it can be seen that with the variation of time-delayed parameters from points Q_1 to Q_2 , two resonance peaks of the MRCs around the first mode are equal. Additionally, the DRCs are getting closer to the MRCs with the decrease of τ_1 and then the two branches merge at Q_2 . From points Q_2 to Q_3 , the two branches separate from each other, thus the equal-peak property is not realized for $0 < \tau_1 < 0.02$. The 3D diagram of FRCs around the second mode in Fig. 5b shows that the equal-peak property is realized and the peak values are almost unaffected by various τ_1 around the second mode.

To analyze the modulation effects of different \mathbf{p}_τ on resonance peaks around the first mode of the beam, three sections of the 3D diagram are given in Fig. 5b when time-delayed parameters are fixed on points Q_1 – Q_3 . The three sections indicate that there are three different cases around the first mode, defined as equal-peak, critical and peak-minimum cases in this study. The reason that the three different cases occurred are

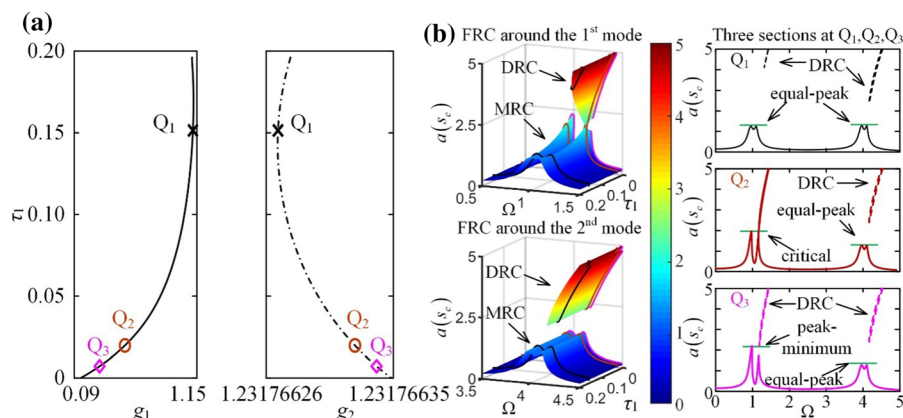


Fig. 5 **a** The time-delayed parameters \mathbf{p}_τ according to Eq. (15) for the first mode at $f = 200$ kN, $\tau_2 = 0.0079636$, **b** 3D diagram of FRCs with the time-delayed parameters in **a** and three sections at points Q_1 – Q_3

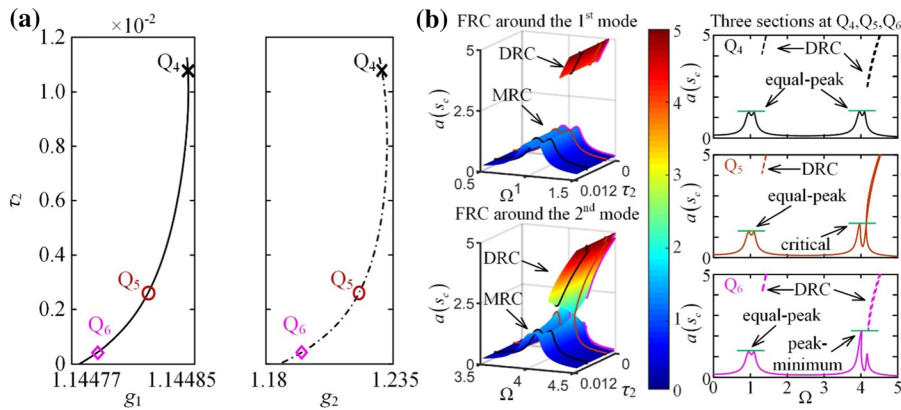


Fig. 6 **a** The time-delayed parameters \mathbf{p}_τ according to Eq. (15) for the second mode at $f = 200$ kN, $\tau_1 = 0.151554$ s, **b** 3D diagram of FRCs with the time-delayed parameters in **a** and three sections at points Q_4 – Q_6

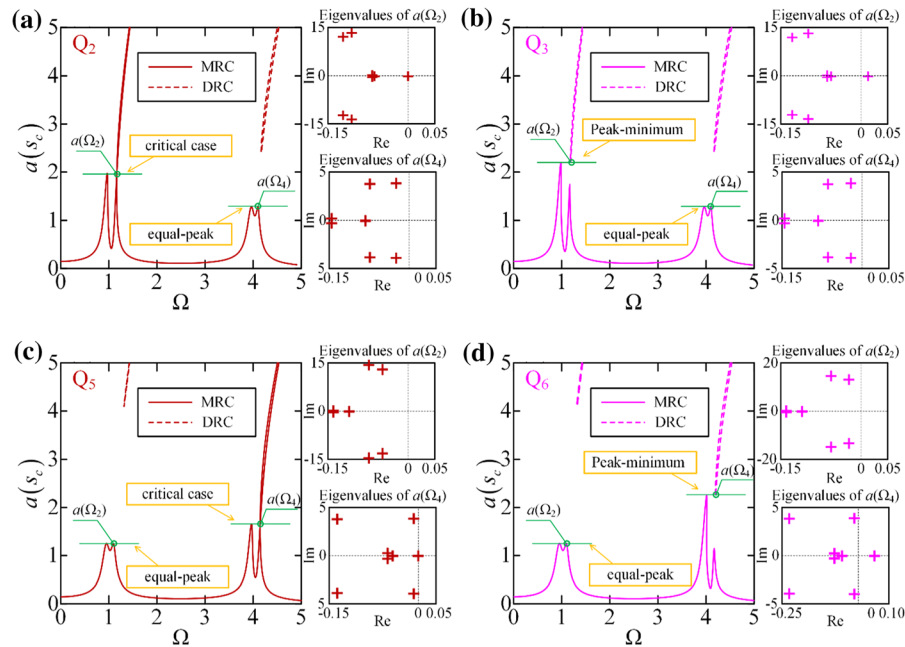


Fig. 7 The FRCs and the eigenvalues at $a(s_c, \mathbf{p}, \mathbf{p}_\tau, \Omega_{2i})$ for **a** point Q_2 , **b** point Q_3 , **c** point Q_5 , **d** point Q_6

given as follows. Following Eq. (13), the extreme points $a(s_c, \mathbf{p}, \mathbf{p}_\tau, \Omega_{2i-1})$, $a(s_c, \mathbf{p}, \mathbf{p}_\tau, \Omega_{2i})$ in frequency domain are calculated by equating the first derivative of the FRC to zero, thus they may either be the local maximum point (peak) of MRC or the local minimum point (minimum) of DRC with the condition $a(s_c, \mathbf{p}, \mathbf{p}_\tau, \Omega_{2i-1}) = a(s_c, \mathbf{p}, \mathbf{p}_\tau, \Omega_{2i})$. Referring to the incremental-iteration procedure in Appendix C with Eq. (15), there are three different cases depending on whether $a(s_c, \mathbf{p}, \mathbf{p}_\tau, \Omega_{2i})$ is a maximum or a minimum

point. In the equal-peak case, $a(s_c, \mathbf{p}, \mathbf{p}_\tau, \Omega_{2i})$ is the second peak of the MRC; in the peak-minimum case, $a(s_c, \mathbf{p}, \mathbf{p}_\tau, \Omega_{2i})$ is the local minimum point of the DRC; in the critical case, the minimum point of DRC merges with the maximum point of MRC. Therefore, the critical case is the boundary between the equal-peak and peak-minimum cases.

In Fig. 6a, the time-delayed parameters are obtained by Eq. (15) for the second mode at $\tau_1 = 0.151554$ s, $f = 200$ kN. The 3D diagram of

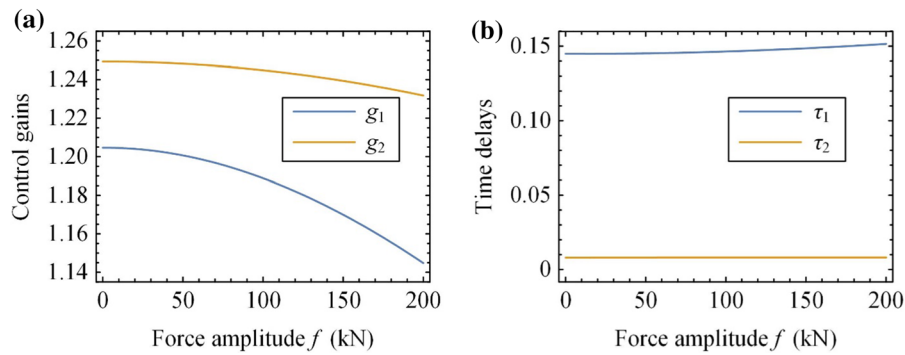


Fig. 8 **a** Optimal control gains for the TDVAs with different force amplitude f , **b** optimal time delays for the TDVAs with different force amplitude f

FRCs in Fig. 6b is obtained with the time-delayed parameters shown in Fig. 6a. With the variation of time-delayed parameters from points Q_4 to Q_6 , the equal-peak property is realized for the first mode as $0 < \tau_2 < 0.011$ and the second mode as $0.0025 < \tau_2 < 0.011$, while it is not realized for the second mode as $0 < \tau_2 < 0.0025$. Thus, three different cases also exist for the second mode. Similar with the cases defined for the first mode, Q_4 , Q_5 and Q_6 are the equal-peak, critical and peak-minimum cases around the second mode, respectively.

Then, the occurrence conditions of the three different cases are analyzed. It discovered from the previous work [39] that for different cases around the i th mode, the second extreme point $a(s_c, \mathbf{p}, \mathbf{p}_\tau, \Omega_{2i})$ has different stability conditions, which could be detected by analyzing its eigenvalues. The characteristic equation of the extreme point $a(s_c, \mathbf{p}, \mathbf{p}_\tau, \Omega_{2i})$ is

$$\det[\mathbf{J}(a(s_c, \mathbf{p}, \mathbf{p}_\tau, \Omega_{2i})) - \lambda \mathbf{I}] = 0, i \in \Psi, \tag{16}$$

where \mathbf{J} is the Jacobian matrix as Eq. (37), \mathbf{I} is the identity matrix and λ is the eigenvalue of the extreme points $a(s_c, \mathbf{p}, \mathbf{p}_\tau, \Omega_{2i})$. Figure 7 shows the FRCs and the corresponding eigenvalues of $a(s_c, \mathbf{p}, \mathbf{p}_\tau, \Omega_2)$ and $a(s_c, \mathbf{p}, \mathbf{p}_\tau, \Omega_4)$ for points Q_2, Q_3 targeted for the first mode and Q_5, Q_6 targeted for the second mode.

From the FRCs of three different cases and eigenvalues of $a(s_c, \mathbf{p}, \mathbf{p}_\tau, \Omega_2)$, $a(s_c, \mathbf{p}, \mathbf{p}_\tau, \Omega_4)$, Fig. 7 shows that for the i th mode, the three different cases relate to different sign of the maximum real part of eigenvalues at the response $a(s_c, \mathbf{p}, \mathbf{p}_\tau, \Omega_{2i})$. The maximum real part of eigenvalue at $a(s_c, \mathbf{p}, \mathbf{p}_\tau, \Omega_{2i})$ is negative, zero and positive for the equal-peak, critical and peak-minimum case around the i th mode,

respectively. Thus, the conditions of three cases around i th mode for nonlinear beams is given as follows

$$\text{Max}\{\text{Real}[\text{eig}[\mathbf{J}(a(s_c, \mathbf{p}, \mathbf{p}_\tau, \Omega_{2i}))]]\} \begin{cases} < 0 & \text{equal-peak,} \\ = 0 & \text{critical case,} \\ > 0 & \text{peak-minimum.} \end{cases} \tag{17}$$

The previous works of equal-peak principle for single modal vibration suppression [19, 24] show that even though the DRC may be induced in nonlinear region, its probability is much less than MRC. Additionally, Figs. 5 and 6 show that for the equal-peak case, the resonance peak of MRC are lower than that of critical and peak-minimum cases, thus time-delayed parameters for the equal-peak case should be selected to suppress the multiple resonances for the nonlinear beam. Therefore, the extremes equal criterion that figures out the equal-peak case is written by combining Eqs. (15 and 17)

$$r_2 = r_{2,a} = \{\mathbf{p}_\tau | a(s_c, \mathbf{p}, \mathbf{p}_\tau, \Omega_{2i-1}) = a(s_c, \mathbf{p}, \mathbf{p}_\tau, \Omega_{2i})\} \cap r_1, i \in \Psi, \text{ subjected to } \{\mathbf{p}_\tau | \text{Max}\{\text{Real}[\text{eig}[\mathbf{J}(a(s_c, \mathbf{p}, \mathbf{p}_\tau, \Omega_{2i}))]]\} < 0\}. \tag{18}$$

The extremes equal criterion Eq. (18) is the second criterion for realizing the multimodal equal-peak principle of nonlinear beams. For degenerated linear systems, the time-delayed parameters \mathbf{p}_τ with first equation in Eq. (18) always lead to the equal-peak case since the DRCs are induced by systems nonlinearity and do not exist in linear systems. However, for nonlinear systems, the first equation in Eq. (18) is insufficient due to the merging phenomena with DRCs and MRCs. The second equation in Eq. (18) is a

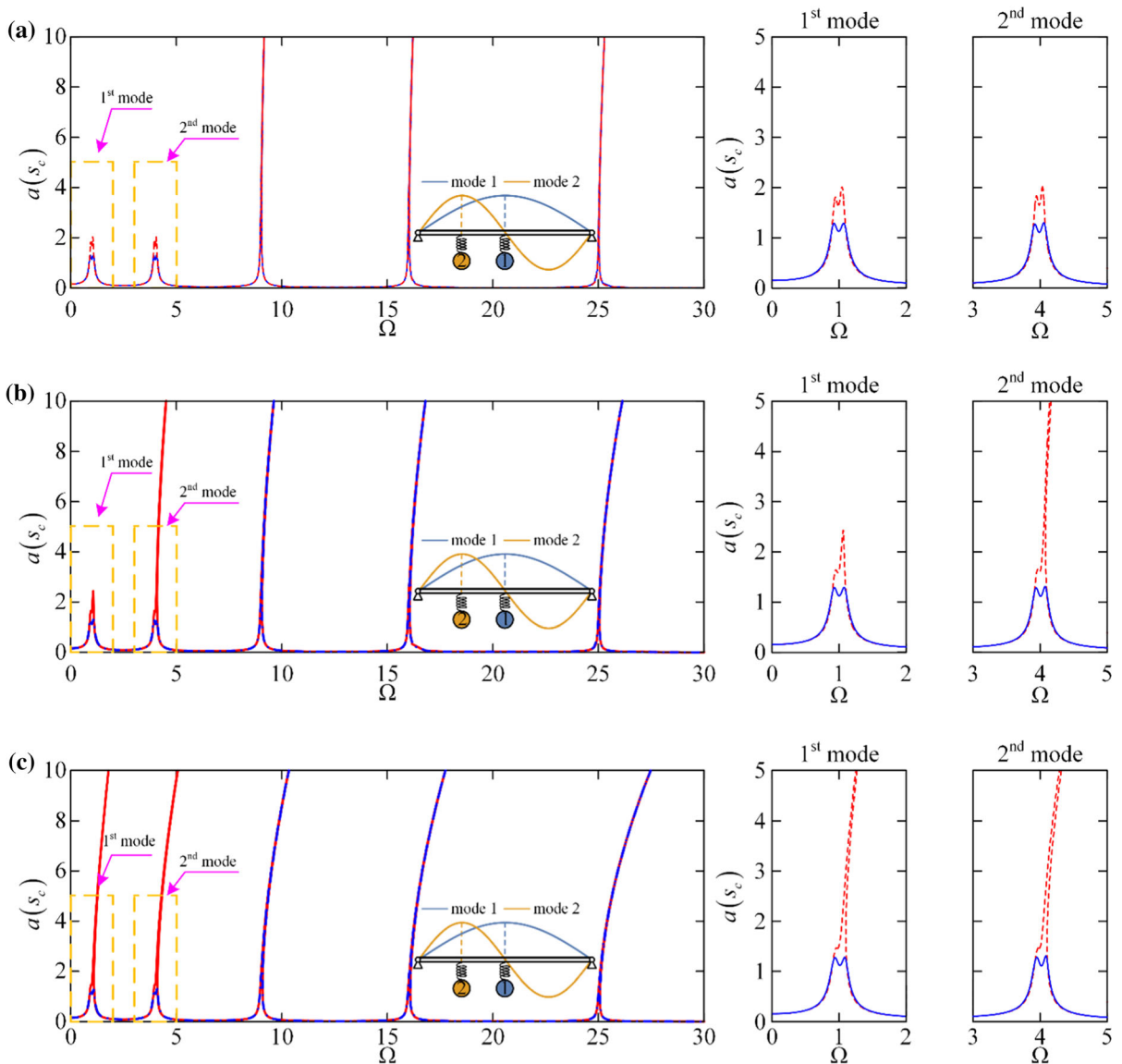


Fig. 9 The FRCs for the nonlinear beam attached by the LTVAs (red dashed lines) and TDVAs (blue lines) at **a** $f = 50$ kN, **b** $f = 100$ kN and **c** $f = 150$ kN. The locations of the two absorbers are $s_1 = l/2$, $s_2 = l/4$, respectively

supplementary condition proposed to distinguish the equal-peak case for the nonlinear systems. Thus, by the extremes equal criterion Eq. (18), the obtained the time-delayed parameters always lead to equal-peak case even for a nonlinear system.

3.3 The minimum peak criterion

In this section, the minimum peak criterion is carried out to figure out the optimal time-delayed parameters

that can suppress the equal peaks around i th mode to the minimum values, which is described as

$$r_3 = \{ \mathbf{p}_\tau | \text{Min}[a(s_c, \mathbf{p}, \mathbf{p}_\tau, \Omega_{2i-1}) = a(s_c, \mathbf{p}, \mathbf{p}_\tau, \Omega_{2i})], \mathbf{p}_\tau \in r_2 \}, i \in \Psi. \tag{19}$$

Eq. (19) is the third criterion for the multimodal equal-peak principle that selects the optimal time-delayed parameters from the equal-peak case determined by the extremes equal criterion Eq. (18). With the minimum peak criterion Eq. (19), the optimal

Table 1 Optimal time delays and the control gains of the two TDVAs for various force amplitudes determined with the minimum peak criterion Eq. (19)

| f (kN) \ g_i, τ_i | g_1 | g_2 | τ_1 | τ_2 |
|--------------------------|--------|--------|----------|----------|
| 50 | 1.2007 | 1.2482 | 0.1457 | 0.00804 |
| 100 | 1.1888 | 1.2449 | 0.1457 | 0.00804 |
| 150 | 1.1700 | 1.2394 | 0.1486 | 0.00804 |

time-delayed parameters for the first and second TDVA with various force amplitudes are shown in Fig. 8 a and b.

From Fig. 8a, it can be seen that the optimal g_1 and g_2 decrease with the increase of force amplitude f and the value of g_1 is less than that of g_2 for fixed force amplitude. Figure 8b shows that with the increase of force amplitude, the optimal τ_1 increases and the optimal τ_2 almost unchanged. By attaching two TDVAs with the optimal time-delayed parameters shown in Fig. 8a and b, the resonance peaks around the first and second modes can be simultaneously suppressed to the equal and minimum values. Therefore, with the proposed three criteria, the multimodal equal-peak principle for the nonlinear multimodal vibration suppression problems is realized.

By applying the proposed multimodal equal-peak principle with the three criteria, the optimal time-delayed parameters of TDVAs are obtained with increasing excitation amplitudes, as shown in Table 1. With the first five modes retained ($P = 5$), Fig. 9 depicts the FRCs of the nonlinear beam attached by the TDVAs with time-delayed parameters shown in Table 1 and the passive LTVAs designed by Eqs. (7 and 9).

As shown in Fig. 9a, b and c, the multimodal vibration suppression effects of LTVAs and TDVAs for the nonlinear beam are compared. For LTVAs at $f = 50$ kN in Fig. 9a, the two peaks slightly diverge for the first and second modes. With the increase of force amplitude to $f = 100$ kN in Fig. 9b and $f = 150$ kN in Fig. 9c, the resonance peaks around the second and the first mode are completely detuned, respectively. Thus, passive LTVAs are not applicable for nonlinear multimodal vibration suppression with increasing

amplitudes. For TDVAs shown in Fig. 9a, b and c, the optimal time-delayed parameters are determined by the proposed principle with three criteria for increasing force amplitude. The optimally designed TDVAs can simultaneously suppress the multimodal nonlinear resonances of the nonlinear beam to the equal and minimum values. Thus, TDVAs and the proposed multimodal equal-peak principle can be applied to suppress the multimodal resonances for the nonlinear beam.

3.4 Vibration suppression for three modes of the nonlinear beam with three TDVAs

In the previous case study, even the peaks around the first two modes are suppressed to the equal and minimum values, the resonance peak around the third mode is still very high since it is not affected by the two TDVAs. To suppress the nonlinear resonance around the third mode, the third absorber is introduced and the concerned modes that need to be suppressed are $\Psi = \{1, 2, 3\}$. The total mass of the three absorbers remains unchanged as $\mu = 0.01$. The i th ($i = 1, 2, 3$) absorber is attached to suppress the resonances around the i th ($i = 1, 2, 3$) mode. Based on the generalized fixed-points theory for LTVAs as Eqs. (7) and (9), their structural parameters are obtained and listed in Table 2, thus $\mathbf{p}_0 = \{\beta_1^0, \beta_2^0, \beta_3^0, \gamma_1^0, \gamma_2^0, \gamma_3^0, f\} = \{0.9814, 3.9962, 8.9988, 0.08349, 0.01895, 0.007092, 0 \sim 10^5\}$. For the TDVAs, the structural parameters are no longer limited by the design rule for LTVAs as Eqs. (7) and (9) since the actively introduced time-delayed feedback can tune the equivalent stiffness and damping properties of the

Table 2 Structural parameters of the LTVAs

| LTVAs | μ_1^0 | μ_2^0 | μ_3^0 | γ_1^0 | γ_2^0 | γ_3^0 | β_1^0 | β_2^0 | β_3^0 |
|-------|-----------|-----------|------------|--------------|--------------|--------------|-------------|-------------|-------------|
| Value | 0.009454 | 0.000479 | 0.00006706 | 0.08349 | 0.01895 | 0.007092 | 0.9814 | 3.9962 | 8.9988 |

Table 3 Optimal time delays and the control gains of the three TDVAs for various force amplitudes determined by the minimum peak criterion Eq. (19)

| $f(\text{kN}) \backslash g_i, \tau_i$ | g_1 | g_2 | g_3 | τ_1 | τ_2 | τ_3 |
|---------------------------------------|---------|---------|---------|----------|----------|----------|
| 50 | 1.20032 | 1.24769 | 1.24874 | 0.11356 | 0.006275 | 0.00105 |
| 100 | 1.18838 | 1.24433 | 1.24703 | 0.11445 | 0.006285 | 0.00105 |
| 150 | 1.16922 | 1.23880 | 1.24422 | 0.11625 | 0.006295 | 0.00104 |

absorbers. In this case, the mass ratio of each TDVA is assumed the same as the LTVAs, while the stiffness and damping coefficients are $\mathbf{p} = \{\beta_1, \beta_2, \beta_3, \gamma_1, \gamma_2, \gamma_3, f\} = \{1.5\beta_1^0, 1.5\beta_2^0, 1.5\beta_3^0, 0.45\gamma_1^0, 0.45\gamma_2^0, 0.45\gamma_3^0, 0 \sim 10^5\}$. By adopting the similar procedure and the steps shown in Appendix C, the structural parameters of TDVAs in this case are updated from the values of \mathbf{p}_0 to \mathbf{p} . The optimal time-delayed parameters of TDVAs for structural parameter coefficients \mathbf{p} are determined and shown in Table 3 for various excitation amplitudes. With the first five modes retained ($P = 5$), Fig. 10 shows the FRCs of the nonlinear beam attached by three TDVAs and three LTVAs designed by Eqs. (7) and (9).

As shown in Fig. 10a, b and c, FRCs are given for the nonlinear beam controlled by LTVAs with the parameters in Table 2 and TDVAs with the optimal time-delayed parameters in Table 3 for various force amplitudes. For the LTVAs at $f = 50$ kN in Fig. 10a, the two peaks are slightly different for the first three modes. At $f = 100$ kN in Fig. 10b, the peaks around the second and third modes are completely detuned. At $f = 150$ kN in Fig. 10c, only one peak with high value exists for the first, second and third modes. Thus, the passive LTVAs cannot be applied to suppress the

multiple resonances for the nonlinear beam with increasing force amplitude. While for TDVAs with increasing force amplitude, the optimal time-delayed parameters are determined by the proposed principle with three criteria. As shown in Fig. 10a, b and c, the optimally designed TDVAs simultaneously suppress the multiple resonance peaks of the nonlinear beam to the equal and minimum values for various force amplitudes. Thus, the TDVAs are more beneficial for realizing the multimodal equal-peak optimization objective for suppressing the nonlinear multimodal vibration of the nonlinear beam.

4 Conclusions

In this study, multiple TDVAs are applied to suppress the multiple resonances of the nonlinear beam. The optimal time-delayed parameters of the TDVAs are obtained by the proposed multimodal equal-peak principle with three criteria. First, with the stability criterion, the time-delayed parameters are restricted in the region in which the equilibrium is stable. Then, the extremes equal criterion is proposed to ensure two resonance peaks around each mode are equal. Next,

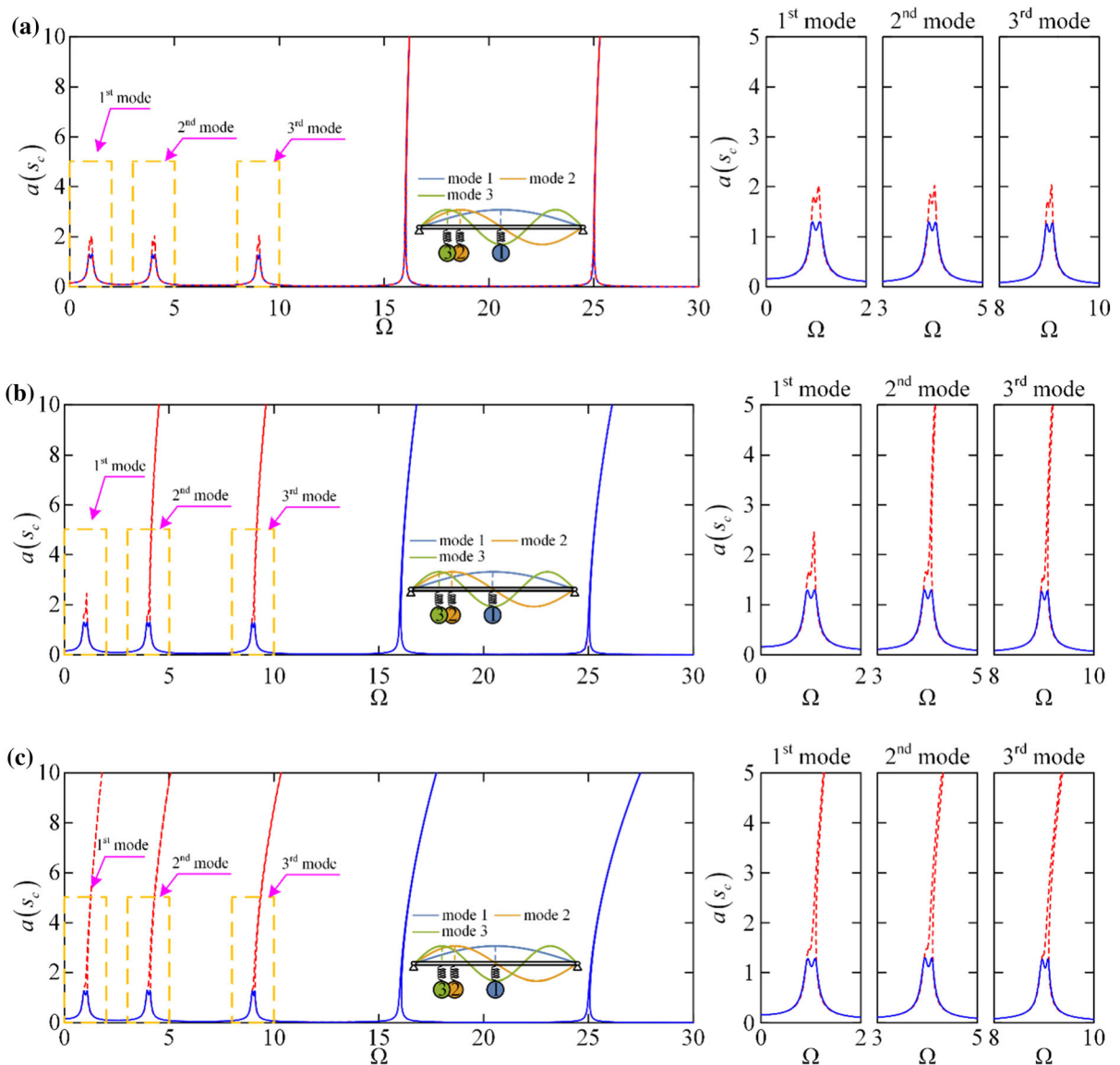


Fig. 10 The FRCs for the nonlinear beam attached by the LTVAs (red dashed lines) and TDVAs (blue lines) at **a** $f = 50$ kN, **b** $f = 100$ kN and **c** $f = 150$ kN. The locations of the three absorbers are $s_1 = 1/2$, $s_2 = 1/4$, $s_3 = 1/6$, respectively

the minimum peak criterion is established to figure out the optimal time-delayed parameters that suppress the peaks around multiple modes to equal and minimum values. Finally, two case studies for suppressing the nonlinear resonances around two and three modes are given. The results show that the optimally designed TDVAs simultaneously suppress the multiple nonlinear resonance peaks of the beam to the equal and minimum values for increasing force amplitude.

Besides, compared with the passive LTVAs for the same mass ratio, the resonance peaks of the beam with TDVAs are suppressed to much lower levels and the effective working band of the force amplitude is extended to a broader range.

In summary, with the proposed multimodal equal-peak principle, TDVAs can realize the beneficial performance for multimodal vibration suppression of the nonlinear beam. Thus, the proposed TDVAs and

the multimodal equal-peak principle have remarkable application prospects in nonlinear vibration suppression fields under excitations with broad frequency band and large amplitude, such as the civil engineering and aerospace.

Acknowledgements The authors would like to gratefully acknowledge the support from the National Natural Science Foundation of China under Grants No. 11772229, 11972254 and 11932015.

Declarations

Conflict of interest The authors declare that they have no conflict of interest.

Appendix A

The Galerkin truncation is adopted to discretize the partial differential equation Eq. (1), the deflection of the beam can be represented by a finite sum as

$$w(s, t) \approx \sum_{p=1}^P \phi_p(s) q_p(t), \tag{20}$$

where P is the number of modes retained. $q_p(t)$ and $\phi_p(s)$ are the p th generalized coordinate and mode shape function. For hinged-hinged supported beam, the mode shape function is given as follow

$$\phi_p(s) = \sqrt{2} \sin\left(\frac{p\pi s}{l}\right). \tag{21}$$

The mode shape function satisfies the orthogonality conditions as

$$\int_0^l \rho A \phi_{p_1}(s) \phi_{p_2}(s) ds = \begin{cases} \rho Al, & p_1 = p_2, \\ 0, & p_1 \neq p_2. \end{cases} \tag{22}$$

Assuming the beam is subjected to the harmonic concentrated excitation with amplitude f and frequency Ω

$$F_e = f \cos(\Omega t). \tag{23}$$

Substituting Eq. (20) into Eq. (1), multiplying both sides by the mode function $\phi_p(s)$, then integrating the result along the length of the beam l , one can obtain $P + N$ Galerkin-reduced equations

$$\begin{aligned} & M_p \ddot{q}_p + C_p \dot{q}_p + K_p q_p \\ & - \int_0^l \left\{ \frac{EA}{2I} \left[\int_0^l \left(\sum_{p=1}^P \phi_p'(s) q_p \right)^2 ds \right] \sum_{p=1}^P \phi_p''(s) q_p \right\} \phi_p(s) ds \\ & + \sum_{i=1}^P m_i \ddot{v}_i(t) \phi_p(s_i) = F_p, \quad p = 1, 2, \dots, P, \\ & m_i \ddot{v}_i + k_i \left[v_i - \sum_{p=1}^P \phi_p(s_i) q_p \right] + c_i \left[\dot{v}_i - \sum_{p=1}^P \phi_p(s_i) \dot{q}_p \right] \\ & - g_i v_i(t - \tau_i) = 0, \quad i = 1, 2, \dots, N, \end{aligned} \tag{24}$$

where the p th modal mass, damping, stiffness and force are

$$\begin{aligned} M_p &= \int_0^l \rho A \phi_p^2(s) ds, \\ C_p &= \int_0^l c \phi_p^2(s) ds, \\ K_p &= \int_0^l EI \left[\phi_p''(s) \right]^2 ds = \int_0^l EI \phi_p''''(s) \phi_p(s) ds, \\ F_p &= f \cos(\Omega t) \phi_p(s_f). \end{aligned} \tag{25}$$

Introducing the dimensionless transform parameters as.

$$\begin{aligned} \bar{t} = \bar{\omega}_1 t &= \sqrt{\frac{K_1}{M_1}} t, \bar{x}_p = \frac{q_p K_1}{f}, \bar{y}_i = \frac{v_i K_1}{f}, \bar{\omega}_p = \sqrt{\frac{K_p}{M_p}} = \\ \sqrt{\frac{K_p}{M_1}}, \bar{\eta}_i &= \sqrt{\frac{k_i}{m_i}}, \bar{\zeta}_p = \frac{C_p}{2\sqrt{M_1 K_1}}, \bar{\gamma}_i = \frac{c_i}{2\sqrt{m_i k_i}}, \bar{\lambda}_p = \frac{\bar{\omega}_p}{\bar{\omega}_1}, \\ \bar{\beta}_i &= \frac{\bar{\eta}_i}{\bar{\omega}_1}, \bar{\mu}_i = \frac{m_i}{M_1}, \bar{\tau}_i = \omega_1 \tau_i, \bar{\Omega} = \frac{\Omega}{\omega_1}, \bar{g}_i = \frac{g_i}{\bar{\mu}_i K_1}, \end{aligned}$$

substituting the above dimensionless parameters into Eq. (24), then dropping the bar of the dimensionless symbols $\bar{t}, \bar{x}_p, \bar{y}_i, \bar{\omega}_p, \bar{\eta}_i, \bar{\zeta}_p, \bar{\gamma}_i, \bar{\lambda}_p, \bar{\beta}_i, \bar{\mu}_i, \bar{\tau}_i, \bar{\Omega}$ and \bar{g}_i for convenience, we can derive Eq. (2).

For $P = 2, N = 2$ in the case from Sect. 3.1 to Sect. 3.3, the matrix and vector of Eq. (4) are

$$\mathbf{M} = \begin{bmatrix} 1 & 0 & \mu_1 \phi_1(s_1) & \mu_2 \phi_1(s_2) \\ 0 & 1 & \mu_1 \phi_2(s_1) & \mu_2 \phi_2(s_2) \\ 0 & 0 & 1 & 0 \\ 0 & 0 & 0 & 1 \end{bmatrix}, \tag{26}$$

$$\mathbf{C} = \begin{bmatrix} 2\zeta_1 & 0 & 0 & 0 \\ 0 & 2\zeta_2 & 0 & 0 \\ -2\beta_1 \gamma_1 \phi_1(s_1) & -2\beta_1 \gamma_1 \phi_2(s_1) & 2\beta_1 \gamma_1 & 0 \\ -2\beta_2 \gamma_2 \phi_1(s_2) & -2\beta_2 \gamma_2 \phi_2(s_2) & 0 & 2\beta_2 \gamma_2 \end{bmatrix}, \tag{27}$$

$$\mathbf{K} = \begin{bmatrix} \lambda_1^2 & 0 & 0 & 0 \\ 0 & \lambda_2^2 & 0 & 0 \\ -\beta_1^2 \phi_1(s_1) & -\beta_1^2 \phi_2(s_1) & \beta_1^2 & 0 \\ -\beta_2^2 \phi_1(s_2) & -\beta_2^2 \phi_2(s_2) & 0 & \beta_2^2 \end{bmatrix}, \tag{28}$$

$$\mathbf{F}_n = [f_{nl,1} \quad f_{nl,2} \quad 0 \quad 0]^T, \tag{29}$$

$$\mathbf{X} = [x_1 \quad x_2 \quad y_1 \quad y_2]^T, \tag{30}$$

$$\mathbf{F} = [\phi_1(s_f) \cos(\Omega t) \quad \phi_2(s_f) \cos(\Omega t) \quad 0 \quad 0]^T. \tag{31}$$

The last matrix on the left side of Eq. (11) is

$$\mathbf{G}_\tau(\mathbf{p}_\tau) = \begin{pmatrix} 0 & 0 & 0 & 0 \\ 0 & 0 & 0 & 0 \\ 0 & 0 & -g_1 \lambda_1^2 e^{-s\tau_1} & 0 \\ 0 & 0 & 0 & -g_2 \lambda_2^2 e^{-s\tau_2} \end{pmatrix}. \tag{32}$$

Appendix B

The Averaging Method is adopted to derive the approximate steady-state harmonic response of Eq. (2). The approximate solution is assumed as

$$\begin{cases} x_p = A_{p,1} \cos(\Omega t) + A_{p,2} \sin(\Omega t) \\ \dot{x}_p = -A_{p,1} \Omega \sin(\Omega t) + A_{p,2} \Omega \cos(\Omega t) \end{cases}, \quad p = 1, 2, \dots, P, \\ \begin{cases} y_i = B_{i,1} \cos(\Omega t) + B_{i,2} \sin(\Omega t) \\ \dot{y}_i = -B_{i,1} \Omega \sin(\Omega t) + B_{i,2} \Omega \cos(\Omega t) \end{cases}, \quad i = 1, 2, \dots, N, \tag{33}$$

where $A_{p,1}, A_{p,2}, B_{i,1}, B_{i,2}$ are slow-varying functions of t . Substituting Eq. (33) into Eq. (2), reducing the trigonometric function and dropping the higher-order harmonic terms, then equating the coefficients of sine and cosine terms to zero, one can derive the amplitude modulation equations

$$\mathbf{v}' = \Gamma(\mathbf{v}, \Omega, \mathbf{p}, \mathbf{p}_\tau), \tag{34}$$

where $\mathbf{v} = \{A_{p,1}, A_{p,2}, B_{i,1}, B_{i,2}\}^T$, $\mathbf{p}_\tau = \{g_i, \tau_i\}$, $p = 1, 2, \dots, P$, $i = 1, 2, \dots, N$. The response of the system can be obtained by solving the equation

$$\Gamma(\mathbf{v}, \Omega, \mathbf{p}, \mathbf{p}_\tau) = 0. \tag{35}$$

The non-dimensional frequency response curve (FRC) of the beam at the location point s_c is

$$a(s_c) = \sqrt{\left(\sum_{p=1}^P A_{p,1} \phi_p(s_c)\right)^2 + \left(\sum_{p=1}^P A_{p,2} \phi_p(s_c)\right)^2}. \tag{36}$$

The stability of the steady-state solution is determined by the corresponding eigenvalues of the Jacobian matrix. The Jacobian matrix of Eq. (34) for the response coefficients \mathbf{v} , time-delayed parameters $\mathbf{p}_\tau = \{g_i, \tau_i\}, i = 1, \dots, N$ at the resonance frequencies Ω is

$$\mathbf{J} = \frac{\partial \Gamma}{\partial \mathbf{v}} = \mathbf{J}(\mathbf{v}, \Omega, \mathbf{p}, \mathbf{p}_\tau). \tag{37}$$

Appendix C

Figure 11 shows the procedure of realizing the multimodal equal-peak principle for nonlinear multimodal vibration suppression. In Fig. 11, \mathbf{p}_0 is structural parameters of LTVAs designed by the generalized fixed-points theory as Eqs. (7) and (9), \mathbf{p} is structural parameters of TDVAs that may be different from \mathbf{p}_0 due to some designable requirements in practical, \mathbf{p}_τ is the time-delayed parameters of the TDVAs, \mathbf{R} is the harmonic coefficients at all the resonance frequencies, P is the modes retained for the nonlinear beam and N is the number of the TDVAs with $N \leq P$. By applying the procedure as Fig. 11, the optimal \mathbf{p}_τ with the minimum peaks around the concerned modes are obtained for the structural parameters of the TDVA \mathbf{p} with increasing force amplitudes f . The main steps of the procedure are shown as follows:

Step 0: Start the optimization procedure.

Step 1: For $f = 0$, the beam degenerates into a linear one, the LTVAs with the structural parameters determined by Eqs. (7) and (9), the initial time-delayed parameters $\mathbf{p}_\tau = 0$, can suppress the peaks for the first two modes to the equal values (see Fig. 3a for details). For the case from Sect. 3.1 to 3.3, the structural parameters of the LTVAs are

$$\mathbf{p}_0 = \{\beta_1^0, \beta_2^0, \gamma_1^0, \gamma_2^0, f\} = \{0.9813, 3.9962, 0.0838, 0.019, 0\}. \tag{38}$$

The vector in Eq. (38) are selected as the initial structural parameters of TDVAs. The initial responses

Algorithm: The procedure of multiple equal-peak principle for multimodal vibration suppression

Input: structural parameters of TDVAs \mathbf{p} , initial parameters of LTVAs \mathbf{p}_0 ,
 number of TDVAs $N (N \leq P)$, initial time-delayed parameters $\mathbf{p}_\tau = 0$,
 initial harmonic coefficients \mathbf{R} at all the resonance frequencies.
for $k=1$ to k_t **do** (*update the structural parameters vector from \mathbf{p}_0 to \mathbf{p} in k_t steps*)
 $\mathbf{p}_{k+1} = \mathbf{p}_k + \Delta \mathbf{P}$
 for $i=1$ to N (*update \mathbf{p}_τ and \mathbf{R} targeted for the i^{th} mode*)
 Compute the eigenvalues s of the linear system by Eq. (11)
 If the stability condition as Eq. (12) is not satisfied **then**
 Break
 end
 Compute the eigenvalues of the response $a(s_c, \mathbf{p}, \mathbf{p}_\tau, \Omega_{2i})$ as Eq. (16)
 If $\text{Max}\{\text{Real}[\text{eig}[\mathbf{J}(a(s_c, \mathbf{p}, \mathbf{p}_\tau, \Omega_{2i}))]]\} < 0$
 equal-peak case around the i^{th} mode
 else if $\text{Max}\{\text{Real}[\text{eig}[\mathbf{J}(a(s_c, \mathbf{p}, \mathbf{p}_\tau, \Omega_{2i}))]]\} = 0$
 critical case around the i^{th} mode
 else $\text{Max}\{\text{Real}[\text{eig}[\mathbf{J}(a(s_c, \mathbf{p}, \mathbf{p}_\tau, \Omega_{2i}))]]\} > 0$
 peak-minimum case around the i^{th} mode
 end
 Compute \mathbf{p}_τ that lead to the equal-peak case by the extremes peak condition as Eq. (18)
 Compute the optimal \mathbf{p}_τ with the minimum peaks by the minimum peak condition as Eq. (19)
 Return the optimal \mathbf{p}_τ and corresponding \mathbf{R} as the initial values for the next mode
 end
Return the optimal \mathbf{p}_τ and corresponding \mathbf{R} as the initial values for the next step
end
Output: structural parameters \mathbf{p} , force amplitude f , optimal time-delayed parameters \mathbf{p}_τ ,
 harmonic coefficients at all resonance frequencies \mathbf{R} .

Fig. 11 The incremental-iteration procedure of the multimodal equal-peak principle for multimodal vibration suppression

at all the resonance frequencies are determined by analyzing the degenerated linear system, as

$$\mathbf{R} = \{ \mathbf{v}_1^0, \Omega_1^0, \mathbf{v}_2^0, \Omega_2^0, \mathbf{v}_3^0, \Omega_3^0, \mathbf{v}_4^0, \Omega_4^0 \}, \tag{39}$$

where $\mathbf{v}_i^0, i = 1, 2, 3, 4$ is the vector of harmonic coefficients at the resonance frequency $\Omega_i^0, i = 1, 2, 3, 4$ for the degenerated linear system. The values of the symbols in Eq. (39) are

$$\Omega_1^0 = 0.942472, \Omega_2^0 = 1.0399, \Omega_3^0 = 3.95392, \Omega_4^0 = 4.04211, \tag{40}$$

$$\begin{aligned} \mathbf{v}_1^0 &= \{ 2.55104, 3.63826, -0.0549022, 0.000147676, -12.2292, 33.4645, 2.61703, 3.85413 \}, \\ \mathbf{v}_2^0 &= \{ -1.84668, 3.99843, -0.0558216, 0.000204213, -19.0512, -22.2499, 2.06857, 4.28766 \}, \\ \mathbf{v}_3^0 &= \{ -0.0479816, 0.0356316, -1.20162, -2.03108, 0.0019377, -0.00640033, 35.144, -68.9216 \}, \\ \mathbf{v}_4^0 &= \{ -0.04907, -0.0308489, 1.09542, -2.00446, 0.00620877, -0.000535353, 39.8503, 60.1105 \}. \end{aligned} \tag{41}$$

In this case, the structural parameters of TDVAs are

$$\begin{aligned} \mathbf{p} &= \{\beta_1, \beta_2, \gamma_1, \gamma_2, f\} \\ &= \{1.5\beta_1^0, 1.5\beta_2^0, 0.3\gamma_1^0, 0.3\gamma_2^0, 0 \sim 10^5\}. \end{aligned} \quad (42)$$

The structural parameters of TDVA should be updated from \mathbf{p}_0 to \mathbf{p} in k_i steps, each augmentation is $\Delta\mathbf{p} = (\mathbf{p} - \mathbf{p}_0)/k_i$. The elements $\beta_1, \beta_2, \gamma_1, \gamma_2, f$ are sequentially updated. It should be noted that every update step of the parameters from \mathbf{p}_0 to \mathbf{p} may lead to the divergence of the two peaks around each mode (see Fig. 4 for details). The introduced time-delayed parameters $\mathbf{p}_\tau = \{g_i, \tau_i\}, i = 1, \dots, N$ are calculated in **Step 2** to retune the resonance peaks equally and minimum.

Step 2: In the k th update process of structural parameters, $\mathbf{p}_k = \mathbf{p}_{k-1} + \Delta\mathbf{p}$, where the subscript k indicates the k th iteration. Update the optimal time-delayed parameters \mathbf{p}_τ , the responses at resonance frequencies \mathbf{R} for suppressing the peaks around all the modes concerned as follows:

Step 2.1: Update \mathbf{p}_τ for suppressing the peaks around the i th mode.

Fix τ_j for $j \neq i$, update other parameters in \mathbf{p}_τ by Eq. (14), the resonance peaks around the first mode are tuned equally by the extremes equal condition Eq. (18) and suppressed to the minimum values by the minimum peak condition Eq. (19). Meanwhile, the stability of the equilibrium state should be ensured by the stability condition Eq. (12). The optimal \mathbf{p}_τ and corresponding \mathbf{R} are selected as the initial values for suppressing the resonance peaks around the next mode.

Step 2.2: Repeat **Step 2.1** for other concerned modes, update \mathbf{p}_τ and \mathbf{R} , then obtain the optimal \mathbf{p}_τ for suppressing the peaks around all modes concerned.

Step 3: At the end of k th loop, the structural parameters of TDVAs \mathbf{p}_k , the force amplitudes f , corresponding optimal time-delayed parameters \mathbf{p}_τ are selected as the initial values of $(k + 1)$ th loop and then repeat **Step 2**.

Step 4: End the loop if $k = k_i$ and obtain the structural parameters of TDVAs \mathbf{p} , the optimal time-delayed parameters \mathbf{p}_τ , harmonic coefficients at all resonance frequencies \mathbf{R} with various force amplitudes f .

References

- Gwon SG, Choi DH (2017) Improved Continuum Model for Free Vibration Analysis of Suspension Bridges. *J Eng Mech* 143(7):04017038
- Zhang W (2018) Vibration avoidance method for flexible robotic arm manipulation. *J Franklin Inst* 355(9):3968–3989
- Basta EE, Ghommem M, Emam SA (2020) Vibration suppression and optimization of conserved-mass metamaterial beam. *Int J Non-Linear Mech* 120:103360
- Parseh M, Dardel M, Ghasemi MH, Pashaei MH (2016) Steady state dynamics of a non-linear beam coupled to a non-linear energy sink. *Int J Non-Linear Mech* 79:48–65
- Li H, Laima S, Zhang Q, Li N, Liu Z (2014) Field monitoring and validation of vortex-induced vibrations of a long-span suspension bridge. *J Wind Eng Ind Aerodyn* 124:54–67
- Frandsen JB (2001) Simultaneous pressures and accelerations measured full-scale on the Great Belt East suspension bridge. *J Wind Eng Ind Aerodyn* 89(1):95–129
- Larsen A, Eisdahl S, Andersen JE, Vejrum T (2000) Storebælt suspension bridge-vortex shedding excitation and mitigation by guide vanes. *J Wind Eng Ind Aerodyn* 88(2–3):283–296
- Wallace AAC (1985) Wind influence on Kessock bridge. *Eng Struct* 7(1):18–22
- Fujino Y, Yoshida Y (2002) Wind-Induced Vibration and Control of Trans-Tokyo Bay Crossing Bridge. *J Struct Eng* 128(8):1012–1025
- Frahm H (1909) Device for damping vibrations of bodies. USA Patent
- Hartog JPD (1934) *Mechanical Vibrations*, vol 179. McGraw-Hill, New York
- Ormondroyd J, Den Hartog JP (1928) The theory of the dynamic vibration absorber. *Trans ASME, J Appl Mech* 50(7):9–22
- Deraemaeker A, Soltani P (2016) A short note on equal peak design for the pendulum tuned mass dampers. *Proceedings of the Institution of Mechanical Engineers, Part K: J Multi-body Dyn* 231(1):285–291
- Cheng Z, Palermo A, Shi Z, Marzani A (2020) Enhanced tuned mass damper using an inertial amplification mechanism. *J Sound Vib* 475:115267
- Asami T, Nishihara O (2003) Closed-form exact solution to H_∞ optimization of dynamic vibration absorbers (application to different transfer functions and damping systems). *J Vib Acoust* 125(3):398–405
- Hua Y, Wong W, Cheng L (2018) Optimal design of a beam-based dynamic vibration absorber using fixed-points theory. *J Sound Vib* 421:111–131
- Shen Y, Xing Z, Yang S, Sun J (2019) Parameters optimization for a novel dynamic vibration absorber. *Mech Syst Signal Process* 133:106282
- Habib G, Detroux T, Vigié R, Kerschen G (2015) Non-linear generalization of Den Hartog's equal-peak method. *Mech Syst Signal Process* 52–53:17–28
- Habib G, Kerschen G (2016) A principle of similarity for nonlinear vibration absorbers. *Physica D* 332:1–8
- Detroux T, Habib G, Masset L, Kerschen G (2015) Performance, robustness and sensitivity analysis of the nonlinear

- tuned vibration absorber. *Mech Syst Signal Process* 60–61:799–809
21. Sun X, Xu J, Wang F, Cheng L (2019) Design and experiment of nonlinear absorber for equal-peak and de-nonlinearity. *J Sound Vib* 449:274–299
 22. Zhu X, Chen Z, Jiao Y (2018) Optimizations of distributed dynamic vibration absorbers for suppressing vibrations in plates. *J Low Freq Noise, Vib Act Control* 37(4):1188–1200
 23. Raze G, Kerschen G (2019) All-equal-peak design of multiple tuned mass dampers using norm-homotopy optimization.
 24. Raze G, Kerschen G (2020) Multimodal vibration damping of nonlinear structures using multiple nonlinear absorbers. *Inter J Non-Linear Mech* 119:103308
 25. Kitis L, Wang BP, Pilkey WD (1983) Vibration reduction over a frequency range. *J Sound Vib* 89(4):559–569
 26. Asami T, Baz AM (2001) Analytical Solutions to H_∞ and H_2 Optimization of Dynamic Vibration Absorbers Attached to Damped Linear Systems. *Trans Japan Soc Mech Eng* 67(655):597–603
 27. Olgac N, Holm-Hansen BT (1994) A novel active vibration absorption technique: delayed resonator. *J Sound Vib* 176(1):93–104
 28. Hosek M, Elmali H, Olgac N (1997) A tunable torsional vibration absorber: the centrifugal delayed resonator. *J Sound Vib* 205(2):151–165
 29. Zhao Y-Y, Xu J (2007) Effects of delayed feedback control on nonlinear vibration absorber system. *J Sound Vib* 308(1):212–230
 30. Xu J, Sun Y (2015) Experimental studies on active control of a dynamic system via a time-delayed absorber. *Acta Mech Sin* 31(2):229–247
 31. Sun Y, Xu J (2015) Experiments and analysis for a controlled mechanical absorber considering delay effect. *J Sound Vib* 339:25–37
 32. Olgac N, Elmali H, Vijayan S (1996) Introduction to the dual frequency fixed delayed resonator. *J Sound Vib* 189(3):355–367
 33. Olgac N, Jalili N (1998) Modal analysis of flexible beams with delayed resonator vibration absorber: theory and experiments. *J Sound Vib* 218(2):307–331
 34. Jalili N, Olgac N Optimum delayed feedback vibration absorber for MDOF mechanical structures. In: *Proceedings of the 37th IEEE Conference on Decision and Control Tampa, Florida USA, 1999*. pp 4734–4739 vol.4734
 35. Wang F, Xu J (2019) Parameter design for a vibration absorber with time-delayed feedback control. *Acta Mechanica Sinica*
 36. Wang, F., et al., Time-delayed Feedback Control Design and its Application for Vibration Absorption. *IEEE Trans Ind Electron*. 2020: p. 1–1.
 37. Wang F, Sun X, Meng H, Xu J (2020) Time-delayed Feedback Control Design and its Application for Vibration Absorption. *IEEE Trans Ind Electron PP* (99):1–1
 38. Vyhlídal T, Pilbauer D, Alikoç B, Michiels W (2019) Analysis and design aspects of delayed resonator absorber with position, velocity or acceleration feedback. *J Sound Vib*. 459:114831
 39. Meng H, Sun X, Xu J, Wang F (2020) The generalization of equal-peak method for delay-coupled nonlinear system. *Physica D: Nonlinear Phenomena*:132340
 40. Casalotti A, El-Borgi S, Lacarbonara W (2018) Metamaterial beam with embedded nonlinear vibration absorbers. *Int J Non-Linear Mech* 98:32–42

Publisher's Note Springer Nature remains neutral with regard to jurisdictional claims in published maps and institutional affiliations.